Available online at www.sciencedirect.com

ScienceDirect

Ceramics International 40 (2014) 2809–2817

CERAMICS INTERNATIONAL

www.elsevier.com/locate/ceramint

Effects of particulate metallic phase on microstructure and mechanical properties of carbide reinforced alumina ceramic tool materials

Zengbin Yin[a,b], Chuanzhen Huang[a,b,*], Bin Zou[a,b], Hanlian Liu[a,b], Hongtao Zhu[a,b], Jun Wang[a,b]

[a] *Centre for Advanced Jet Engineering Technologies (CaJET), School of Mechanical Engineering, Shandong University, Jinan 250061, PR China*
[b] *Key Laboratory of High-efficiency and Clean Mechanical Manufacture (Shandong University), Ministry of Education, PR China*

Received 1 August 2013; received in revised form 17 September 2013; accepted 9 October 2013
Available online 25 October 2013

Abstract

Alumina-based composite ceramic tool materials reinforced with carbide particles were fabricated by the hot-pressing technology. Choice of metallic phase added into the present composite ceramic was based on the distribution of residual stress in the composite. The effects of metallic phase on microstructure and mechanical properties of composites were investigated. The metallic phase could dramatically improve room temperature mechanical properties by refining microstructure, filling pores and enhancing interfacial bonding strength. However, it also led to sharp strength degradation at high temperature because the metallic phase was easier to be oxidized and get soft at high temperature in air. The effects of metallic phase on strengthening and toughening were discussed. The improved fracture toughness of composite with metallic phase was attributed to the lower residual tensile stress in the matrix and the interaction of more effective energy consuming mechanisms, such as crack bridged by particle, crack deflection and intragranular grain failure.

© 2013 Elsevier Ltd and Techna Group S.r.l. All rights reserved.

Keywords: B. Composites; C. Strength; C. Toughness and toughening; D. Al_2O_3

1. Introduction

Alumina ceramics possess some attractive properties of high hardness, chemical stability, excellent wear resistance and high temperature oxidation resistance. These properties make it possible to be applied in the environments of high temperature, wear and corrosive conditions. However, it is brittle at low temperature because of a fundamental lack of dislocation mobility and insufficient slip systems, which seriously limits its application as engineering material. So improving the flexural strength and fracture toughness is crucial for the use of Al_2O_3 ceramics as the cutting tools. In order to solve this problem, many approaches have been proposed. The strength and toughness can be improved either by the manipulation of microstructural features, such as control of grain size and shape (Si_3N_4 self-toughening and ZrO_2 phase transformation toughening) [1,2], or by use of various second phases, e.g., multi-scale particles [3–5], whiskers [6], rare earth oxides [7] and ductile phase [8–9]. Among the various toughening methods, the ductile reinforcement toughening is one of the most promising toughening mechanisms. Many studies [10–15] have shown that the flexural strength and fracture toughness of composite ceramics can be greatly improved by the inclusion of a small quantity of metallic phase (Ni, Mo, Co and Fe).

Microstructure of the current metallic phase toughened ceramics can be classified into two types such as a particulate distribution microstructure and a continuous (or partially continuous) network microstructure. The addition of the particulate metallic phase into a brittle matrix is now well established as a method for increasing toughness, but in many cases the toughening contribution is small. The main limitation to toughening is lack of plastic deformation of the metallic phase [15]. Toughness increment achieved by the continuous (or partially continuous) network of metallic phase is generally higher than that of the particulate metallic phase. However, the materials toughened by the metallic particles have the

---

[*] Corresponding author at: Centre for Advanced Jet Engineering Technologies (CaJET), School of Mechanical Engineering, Shandong University, Jinan 250061, PR China. Tel./fax: +86 531 88396913.

E-mail address: chuanzhenh@sdu.edu.cn (C. Huang).

0272-8842/$ - see front matter © 2013 Elsevier Ltd and Techna Group S.r.l. All rights reserved.
http://dx.doi.org/10.1016/j.ceramint.2013.10.033

advantages of material homogeneity isotropy and particularly better high temperature properties [16].

In the present wok, the micro-scale (W,Ti)C particles, nano-scale TiC particles and the particulate metallic phase were added into the Al_2O_3 matrix in order to fabricate the composite ceramic tool material with high flexural strength and fracture toughness. Choice of metallic phase was based on the distribution of residual stress in the composite. Effects of metallic phase on the room temperature mechanical properties and high temperature flexural strength were investigated. Effects of metallic phase on strengthening and toughening were discussed.

2. Choice of the metallic phase

The level and nature of the internal stresses in the composite is one of the important factors that influence strengthening and toughening [17]. The distribution of residual stress in each phase of the composite ceramic containing metallic phase, which was induced by the mismatch of thermal expansion coefficients, was quite different from that of the composite without metal [18]. The elements Ni, Mo and Co are commonly added into the carbide particles reinforced ceramics due to their good wettability to the carbide particles. The metallic phase is usually distributed at the interface between the matrix and reinforcing particle, so the residual stress in the composite can be calculated according to the four-layer thermal stress model [19]. When cooled from 1650 °C to the room temperature, the distribution of residual stress in each phase of the Al_2O_3-30 vol% (W,Ti)C composites with/without metallic phase was shown in Fig. 1. As the very low content of nano-TiC in the present composite and small difference of thermal expansion coefficient between TiC and Al_2O_3, so the residual stress induced by nano-TiC was ignored.

The residual stress distribution in the composites containing different metal phases is quite different as shown in Fig. 1(a) and (b). This is mainly ascribed to the difference in the mismatch of thermal expansion coefficients among the matrix, reinforcing particle and metallic phase. The coefficient of thermal expansion of Mo is about $4.8 \times 10^{-6}\,K^{-1}$, which is lower than those of Al_2O_3 and (W,Ti)C. It can be seen that large compressive stresses are distributed in the (W,Ti)C particle and Mo layer as shown in Fig. 1(a). The compressive stress can restrain cracks initiation and propagation, which is beneficial for enhancing the flexural strength and fracture toughness of composite ceramics. However, large tensile stress also exists in Al_2O_3 matrix. The tensile stress can accelerate the cracks propagation in the matrix, causing the negative effect on the mechanical properties. The coefficients of thermal expansion of Ni and Co are about $13 \times 10^{-6}\,K^{-1}$, which are higher than those of Al_2O_3 and (W,Ti)C. Although the tensile stress still exists in Al_2O_3 matrix (Fig. 1(b)), the numerical

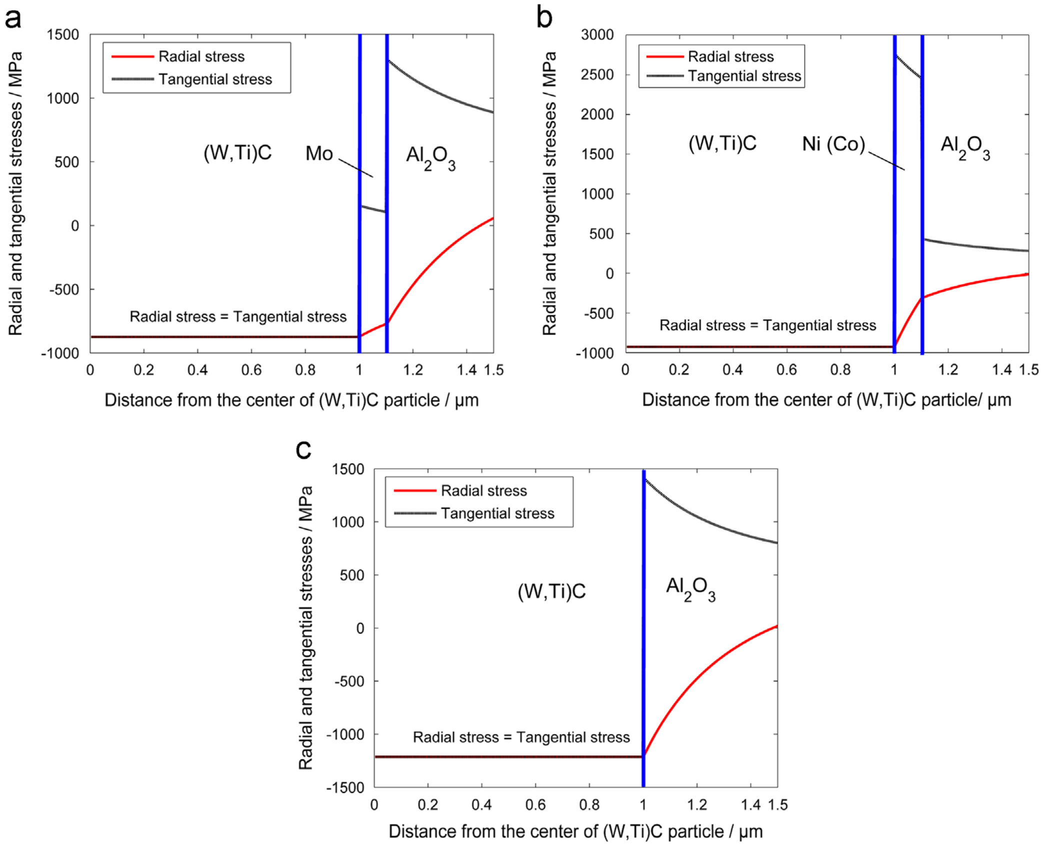

Fig. 1. The distribution of residual stress in the composites with/without metallic phase.

value is much smaller than that in Fig. 1(a). Compared to Fig. 1(c), the tensile stress in the Al_2O_3 matrix of the composite containing Ni or Co is much smaller than that of the composite without the metallic phase. The stress gradient interface can be formed due to the existence of the interphase metallic phase, which is beneficial to decrease the stress concentration and mutation.

In the present work, Ni and Co was added into the composites in order to decrease the tensile stress in the Al_2O_3 matrix and obtain the composite ceramic tool materials with good mechanical properties.

3. Experimental procedures

3.1. Materials preparation

The starting materials were α-Al_2O_3 powders with an average particle size of 0.5 μm (purity: 99.99%, Shanghai, China), nano-scale TiC with an average particle size of 40 nm (purity: 99.9%, Shanghai, China), micro-scale (W,Ti)C (the mass ratio of WC to TiC is 7:3) with an average particle size of 1.5 μm (purity: 99%, Changsha, China) and Ni (or Co) with an average particle size of 2 μm (purity: 99.9%, Shanghai, China). The composition of the composites is shown in Table 1. The nano-scale TiC powders were prepared into suspensions using alcohol as the dispersing medium, and the dispersant PEG (polyethylene glycol, Shanghai, China) was added after ultrasonic dispersion (with SB5200 ultrasonic instrument and D-7401-III motor stirrer, China) for 10 min. The suspensions were dispersed ultrasonically for 20 min after a pH of 9.0 (with PHS-25 digimatic pH-meter, China) was attained by the addition of $NH_3 \cdot H_2O$. After that, the Al_2O_3, (W, Ti)C and the metallic phase were added into the suspensions. The mixed slurries were ball-milled for 48 h, and then dried in a vacuum dry-type evaporator (Moder ZK-82A, China). After that, the dried powders were sieved through a 200-mech sieve for further use. The dried powders were placed into a graphite die and hot-pressed with an applied pressure of 32 MPa at 1650 °C with the holding time of 20–40 min in a vacuum sintering furnace. The composite without metal was sintered at 1650 °C and 1700 °C for 30 min under a pressure of 32 MPa.

Table 1
Composition (vol%) of different composites.

Composite	Al_2O_3	TiC	(W,Ti)C	Ni	Co
A	61	6	33	0	0
AN	57	6	33	4	0
AC	57	6	33	0	4
ANC	57	6	33	2	2

3.2. Characterization

The sintered compacts were cut, ground and polished into specimens with a dimension of 3 mm × 4 mm × 35 mm. The flexural strength was tested using the three-point bending tester (INSTRON 8801, Britain) with a span of 30 mm and a loading velocity of 0.5 mm/min at room temperature 800 °C and 1000 °C in the air, respectively. The samples were soaked at the testing temperature for 10 min to reach a thermal equilibrium. The Vickers hardness was measured on the polished surface using a Vickers diamond pyramid indenter (Model 120, China) with a load of 196 N and a loading holding time of 15 s. The fracture toughness measurement of materials was determined by the Vickers indentation method proposed by Evans and Charles [20]. The relative density of specimens was measured by the Archimedes' method with the distilled water as medium. The fractured surfaces and cracks on the polished surfaces were observed by scanning electron microscopy (SEM, SUPRA-55, ZEISS, Germany). Phase identification was carried out by X-ray diffraction analysis (XRD, RAX-10A X, Hitachi, Japan) with copper $K\alpha$ radiation.

4. Results and discussion

4.1. Mechanical properties and microstructure

4.1.1. Effects of metallic phase on room temperature mechanical properties and microstructure

The XRD patterns of composites AN and AC sintered at 1650 °C for 30 min were shown in Fig. 2. No evidence of any new phases was detected in the XRD spectrum, indicating that there was no chemical reaction among phases during the sintering process.

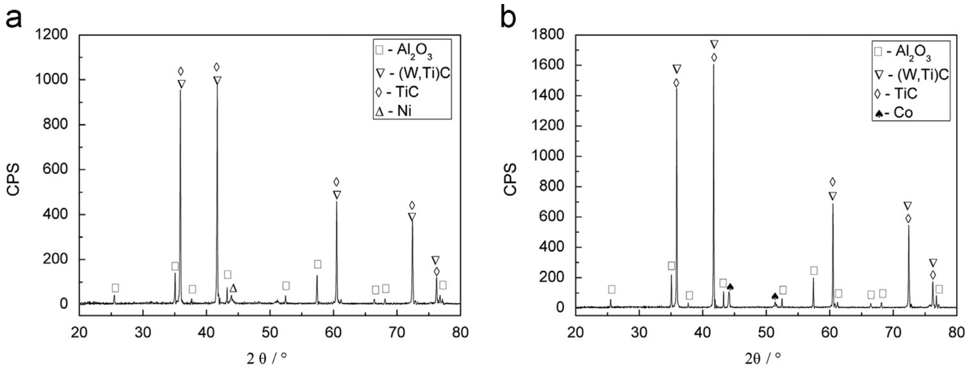

Fig. 2. The XRD patterns of (a) AN and (b) AC at room temperature.

The room temperature flexural strength, fracture toughness and Vickers hardness of the composite without the metallic phase was 554 MPa, 5.12 MPa m$^{1/2}$ and 18.3 GPa, respectively. Fig. 3 showed the room temperature mechanical properties of the composites containing metallic phase sintered at 1650 °C for 20–40 min. The optimal mechanical properties of AN, AC and ANC were obtained when sintered at 1650 °C for 30 min. The flexural strength and fracture toughness of AN, AC and ANC were all much higher than those of the composite without metallic phase. The hardness of AN and ANC was almost equal to that of the composite A, but the hardness of AC was a little higher than that of the composite A.

SEM micrographs of the fractured surfaces of the composites sintered at 1650 °C for 30 min were shown in Fig. 4. For the composite without metallic phase, the microstructure was inhomogeneous with irregular and large grains as shown in Fig. 4(a). There were plenty of pores distributed not only at grain boundaries but also in grains, and the relative density was only 94.8%. The pores can easily cause the stress concentration which promoted cracks initiation around the pores. That was disadvantageous to the flexural strength. Moreover, the relative density was increased to 97.1% when sintered at 1700 °C. However, the mechanical properties were enhanced slightly (a flexural strength of 610 MPa, a fracture toughness of 5.39 MPa m$^{1/2}$ and a Vickers hardness of 19.0 GPa) due to occurrence of abnormal grain growth at higher temperature.

For the composite with Ni or Co, Al_2O_3 and (W,Ti)C particles distributed homogeneously and maintained their original angular shape as shown in Fig. 4(b and c). It indicated that there was no particle clustering, merging and growing during sintering. The grains were much finer than that of the composite without metallic phase. This should be attributed to the metallic phase distributed at grain boundary, which could reduce the free energy of grain boundary, restrain the grain boundary movement and act as grain boundary pinning for grain growth [12]. The relative density was enhanced with the addition of metallic phase, and the relative density of AN and AC were 98.5% and 99.2%, respectively. The melting point Ni and Co was much lower than the sintering temperature. The metal became fluid and filled the pores among grains, thus the composites could possess a high relative density. However, a few pores still existed in composite with Ni as shown in Fig. 4(b). The pores left at the grain boundaries might be ascribed to the poor wettability of Ni to (W,Ti)C at 1650 °C in vacuum. It meant that the Ni liquid phase could not soak into the interfaces of (W, Ti)C particles, thus the gaps among particles could not be fully filled by the liquid phase in the sintering process. This led to a lower flexural strength and hardness than those of the composite with Co. When Ni and Co were simultaneously added into the composite, there were some amorphous phases distributed at the grain boundaries, and the grains were much bigger than that of composite with single metallic phase as shown in Fig. 4(d). Thus some defects were easily congregated inside these abnormally growing grains. The large grains and potential defects existed in the abnormal grains deteriorated the mechanical properties of composite ANC.

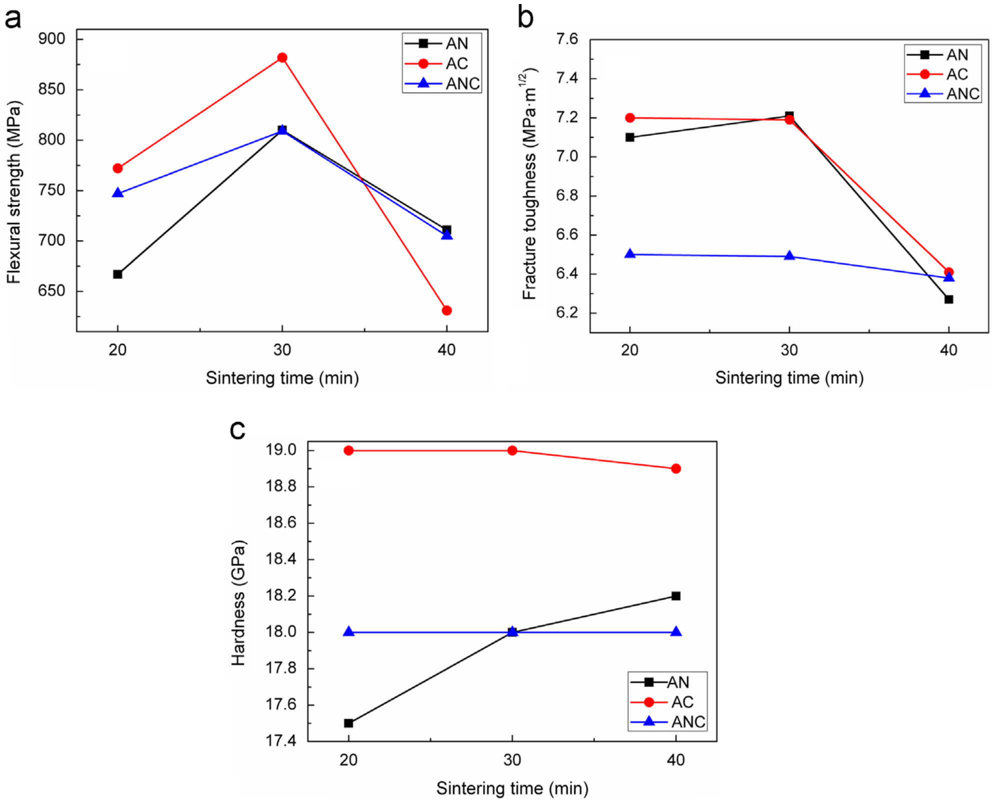

Fig. 3. The ambient temperature (a) flexural strength, (b) fracture toughness and (c) hardness of the composites containing the metallic phase.

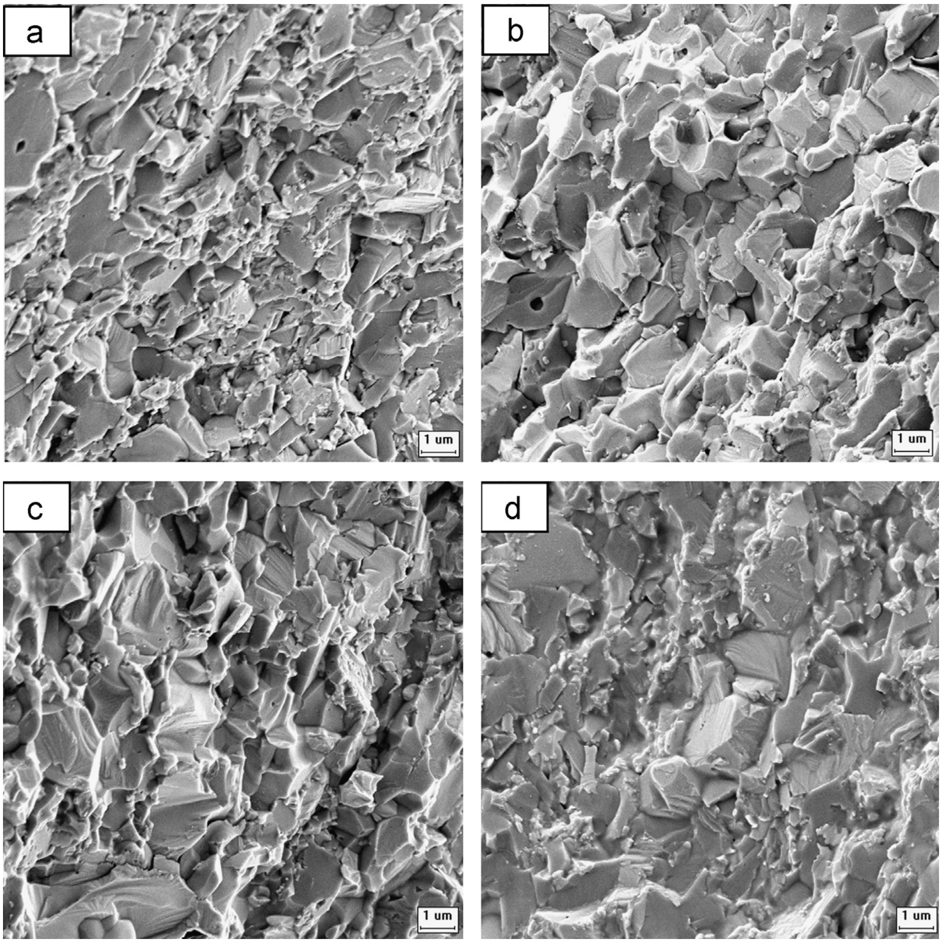

Fig. 4. SEM micrographs of the fractured surfaces of the composites (a) A, (b) AN, (c) AC and (d) ANC sintered at 1650 °C for 30 min.

The presence of metallic phase not only refined the microstructure but also enhanced the interfacial bounding strength, and then led to the change of fracture mode. It can be seen that the fracture mode of the composite without metal was mainly intergranular fracture, indicating a poor interfacial bonding strength. For the composite with Ni or Co, the percentage of transgranular fracture grains was increased. Typical cleavage steps caused by the transgranular fracture were clearly seen, which indicated that the bonding strength between grains was increased and was even higher than the fracture strength of some grains.

4.1.2. *Effects of metallic phase on high temperature flexural strength*

The flexural strength of the composites tested at room temperature, 800 °C and 1000 °C was shown in Fig. 5. The flexural strength of all composites decreased at 800 °C, but still kept a higher value, and the strength of composites with metallic phase was a little higher than that of composite without metal. Compared to the room temperature strength, the flexural strength of all composites decreased sharply at 1000 °C, with the biggest drop in the composites containing metallic phase.

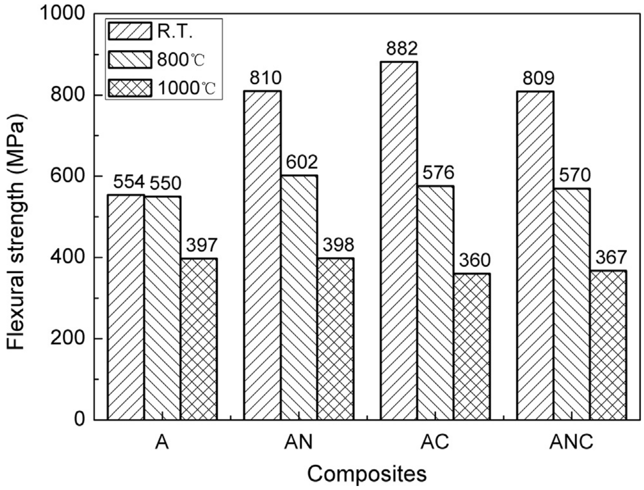

Fig. 5. The flexural strength of the composites tested at room temperature, 800 °C and 1000 °C.

It was well known that the degradation of strength of ceramics at high temperature always related to the softening of grain boundary, i.e., the change of fracture mode as a result of the grain boundary weakness, especially when low melting point phases existed at the grain boundaries [21–23]. Ni or Co distributed at grain boundaries got soft at high temperature, which probably led to the grain boundary having a lower viscosity. The lower viscosity of the grain boundaries resulted in the weakness of the interfacial bonding strength. It meant that cracks preferred to propagate intergranularly and less fracture energy was consumed. This phenomenon was clearly observed in the Al_2O_3–TiC–Co composite ceramic. The fracture mode at 800 °C was mainly intergranular fracture [24]. At 1000 °C, the viscosity of the grain boundary decreased further due to the softening of metallic phase, so the intercrystalline crack propagated more easily and the fracture occurred at low load. In general, the metallic phase had little effects on improving the high temperature strength of ceramics.

Additionally, the strength degradation at high temperature could be ascribed to the oxidation of tension surface, as these tests were carried out in the air. The surface oxidation layer could be easily peeled off after a thermal cycle at 1000 °C. The XRD patterns of the composites tested at 1000 °C were shown in Fig. 6. For the composite without the metallic phase, WC and TiC were oxidized to WO_3 and TiO_2, respectively. The oxides were mainly $NiWO_4$, $CoWO_4$ and TiO_2 in the composites containing metallic phase. A small amount of $CoAl_2O_4$ was detected in the composite containing Co. That was because CoO can react with Al_2O_3 to form $CoAl_2O_4$ at the temperature above 900 °C [25]. For the present composites, the oxygen primarily attacked the metallic phase, then the oxidation of (W,Ti)C and TiC grains occurred. The disappearance of grain boundary phase and the formation of oxides contributed to inducing defects at grain boundaries. The continuous increase of defects progressively propagated towards the bulk material and reduced the area of thrust surface, which induced the strength degradation.

Furthermore, for the composite containing Co, the Al_2O_3 matrix was destroyed except the oxidation of (W,Ti)C grains, which induced the catastrophic degradation of material structure as shown in Fig. 7. This led to the lower high temperature strength than that of composite with Ni.

4.2. Effects of metallic phase on strengthening and toughening

The fracture mode of composites with Ni or Co was a mixture of transgranular and intergranular types, presenting a more complicated fracture mode, which led to the improved flexural strength. The enhanced interface strength due to the presence of Ni or Co distributed along grain boundaries should contribute to the intragranular fracture. Ni or Co restrained the grain boundary movement, resulting in reduced grain size and fine microstructure. The flexural strength increased as the grain size decreased according to Hall–Petch relationship. Meanwhile, the metallic phase enhanced the relative density of composite ceramics, which also benefited mechanical properties.

Compared to the composite without metallic phase, fracture toughness of the composite with Ni or Co was improved by 41%. The possible effects of metallic on toughening were as follows. First, the thermal mismatch between the alumina matrix and (W,Ti)C particles generates a periodic tension-compression residual stress field as shown in Fig. 1. The tangential stress in

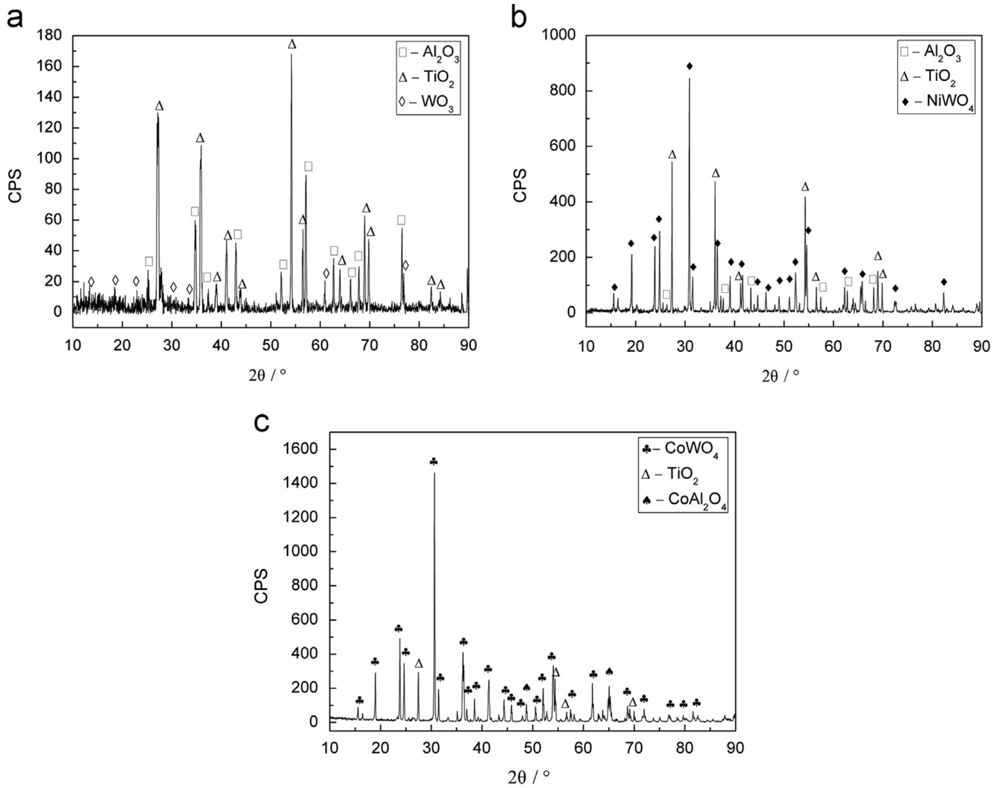

Fig. 6. The XRD patterns of the composites tested at 1000 °C, (a) A, (b) AN and (c) AC.

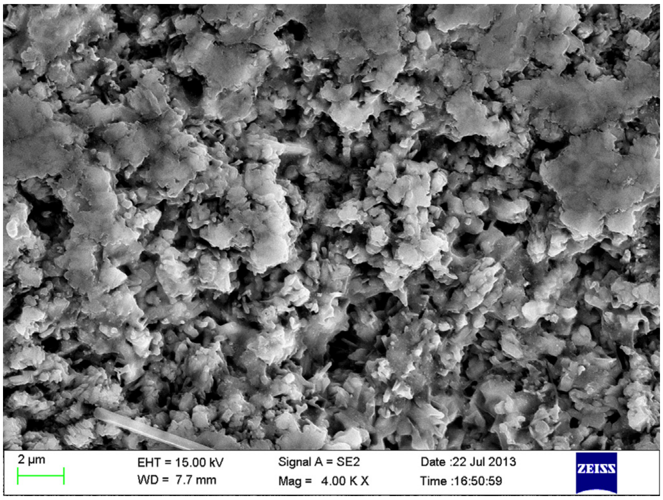

Fig. 7. The tensile surface morphology of composite AC tested at 1000 °C.

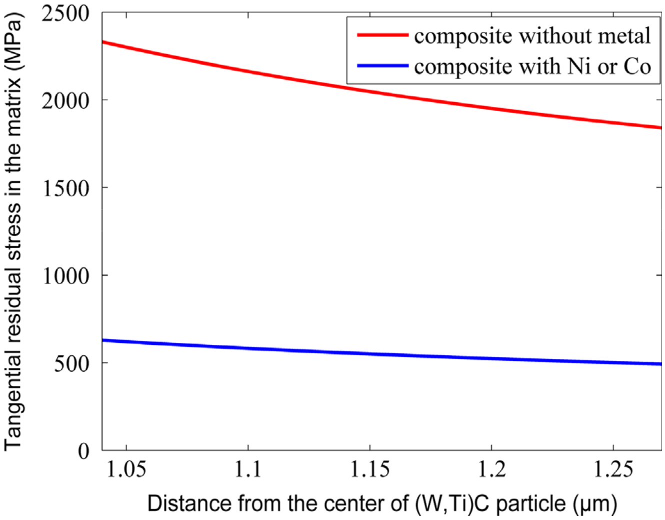

Fig. 8. The distribution of tangential residual stress in the matrix.

the matrix between two adjacent particles is tensile. The tensile residual stress promotes the cracks propagation by increasing the stress intensity factor, and consequently, the toughness is reduced. The toughness reduction can be expressed by [26]

$$\Delta K_T = \sigma_T \times \left(\frac{8\lambda}{\pi}\right)^{1/2} \tag{1}$$

$$\frac{\lambda}{d} = \left(\frac{\pi}{6f_p}\right)^{1/3} \tag{2}$$

where λ is the interparticle distance, d is the particle diameter, f_p is the volume fraction of dispersed particles and σ_T is the tangential residual stress in the matrix. According to the thermal-elastic theory [19,27], σ_T is given by

$$\sigma_T = \frac{a^3(2r^3+b^3)}{2r^3(b^3-a^3)}p_1 - \frac{b^3(2r^3+a^3)}{2r^3(b^3-a^3)}p_2, \frac{a^3}{b^3} = \frac{f_p}{f_m+f_p} \tag{3}$$

where p_1, p_2 are the interfacial residual stresses at the interfaces of metallic phase/matrix and matrix/the equivalent composite, respectively. r is the distance from the center of (W,Ti)C particle.f_p and f_m are the volume fraction of reinforcing particles and matrix.

In the present work, for the composite without metallic phase, p_1 and p_2 are -1213 MPa and 13.7 MPa, respectively, and for the composite with Ni or Co, p_1 and p_2 are -315 MPa and -13.2 MPa, respectively. The distribution of tangential residual stress in the matrix was shown in Fig. 8. The tensile stresses decreased with the increase of r, however, the tensile stress in the composite without metallic phase was much larger than that of the composite with Ni or Co. Therefore, the toughness reduction of the composite with Ni or Co was substantially much smaller than that of the composite without the metallic phase according to Eqs. (1) and (2). So the fracture toughness was improved.

Second, crack in the composite without metallic phase preferred to propagate along the grain boundaries with little deflection as shown in Fig. 9(a). No other toughening mechanism was observed. However, crack bridging and crack deflection played an effective role in improving fracture toughness of the composites with metallic phase.

Crack bridging (denoted with the circles) appeared in the composites containing Ni or Co as shown in Fig. 9(b–d). The black phase was Al_2O_3 and the gray phase was (W,Ti)C. Co element appeared in the EDS spectrum of point A (marked near the interface of Al_2O_3/(W,Ti)C in Fig. 9(b) as shown in Fig. 10, which indicated that the metallic phase tended to locate at grain boundaries. The metallic phase distributed along the grain boundaries can chemically and/or mechanically strength the interface by increasing the interface fracture work [12,17], resulting in an increased interfacial bonding strength. This created the conditions for the anticipated particle bridging. The shielding effect caused by the particle bridging continues until either the particles itself or the particle/matrix interface is first fractured. For the interface fracture, the increase in toughness caused by the particle bridging is given as [26]

$$\Delta K = \frac{\sigma_i \pi^{1/2} d^{1/2}}{4[(\pi/6f_p)+2((\pi/6f_p))^{2/3}]^{1/2}} \tag{4}$$

where σ_i represents the interface fracture strength. Therefore, the presence of crack bridging and the improved interface fracture strength enhanced fracture toughness of the composites containing Ni or Co.

Additionally, crack deflection with large deflection angle (almost 90°) (denoted by red arrows) and intragranular grain failure (denoted by white arrows) were observed in the composites with Ni or Co as shown in Fig. 9(b and c). Thus much fracture energy was consumed during crack propagation and the fracture toughness was increased. Therefore, higher value of fracture toughness should be attributed to the interaction of more effective energy consuming mechanisms in the composite containing metallic phase.

5. Conclusions

(1) There were great differences in the residual stress distribution in the composites containing different metallic phases.

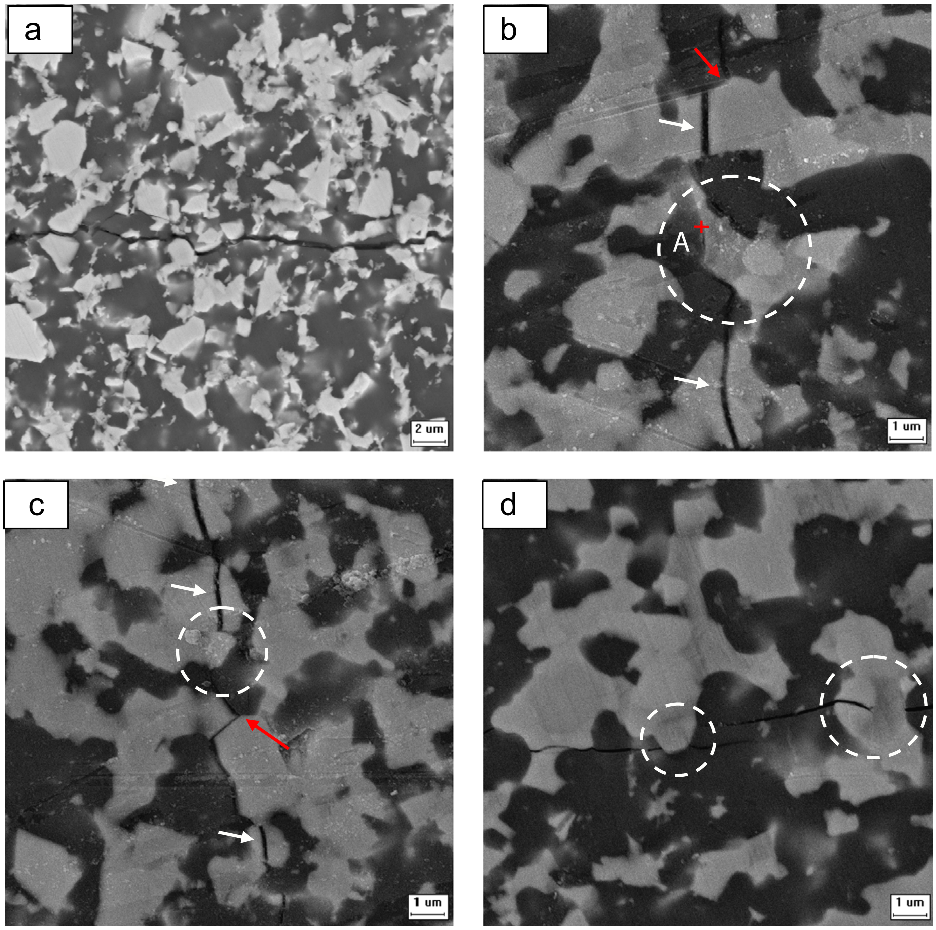

Fig. 9. Vickers indentation crack propagation paths of the composites (a) A, (b)-(c) AC and (d) AN.

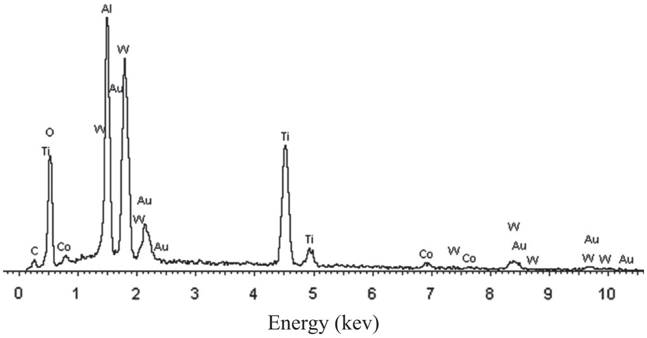

Fig. 10. EDS spectrum of point A marked in Fig. 9(b).

For the composite containing Mo, large compressive stresses existed in (W,Ti)C particle and molybdenum layer. Meanwhile, large tensile stress existed in the Al_2O_3 matrix. However, the tensile stress in the Al_2O_3 matrix of the composites containing Ni or Co was much smaller than those of the composite containing Mo and the composite without the metallic phase.

(2) The metallic phase could dramatically improve the room temperature mechanical properties by refining microstructure, filling pores and enhancing interfacial bonding strength. However, it also led to the sharp strength degradation at high temperature because the metallic phase was easier to be oxidized and get soft at high temperature in air. The ambient temperature mechanical properties of the composite with Co were better than that of the composite with Ni, but it had the biggest drop in the high temperature strength due to its bad resistance to oxidation.

(3) The residual tensile stress in matrix of the composites containing Ni or Co was much lower than that of the composite without metallic phase, which led to a small toughness reduction. Ni or Co distributed at the grain boundaries could enhance the interfacial bonding strength, creating the conditions for crack bridging and crack deflection. So, much crack extension energy was expended by these effective energy consuming mechanisms, and the fracture toughness was enhanced.

Acknowledgements

The work is supported by Key Special Project of Numerical Control Machine Tool (2012ZX04003-051).

References

[1] B. Zou, C.Z. Huang, M. Chen, M.L. Gu, H.L. Liu, Study of the mechanical properties, toughening and strengthening mechanisms of $Si_3N_4/Si_3N_{4w}/TiN$ nanocomposite ceramic tool materials, Acta Mater. 55 (2007) 4193–4202.

[2] Z.M. Zhao, L. Zhang, J. Zheng, H.B. Bai, S.Y. Zhang, B.C. Xu, Microstructures and mechanical properties of Al_2O_3/ZrO_2 composite produced by combustion synthesis, Scr. Mater. 53 (2005) 995–1000.

[3] Y.L. Dong, F.M. Xu, X.L. Shi, C. Zhang, Z.J. Zhang, J.M. Yang, Y. Tan, Fabrication and mechanical properties of nano-/micro-sized Al_2O_3/SiC composites, Mater. Sci. Eng. A 504 (2009) 49–54.

[4] J. Zhao, X.L. Yuan, Y.H. Zhou, Processing and characterization of an Al_2O_3/WC/TiC micro-nano-composite ceramic tool material, Mater. Sci. Eng. A 527 (2010) 1844–1849.

[5] M.R. Cao, S.B. Wang, W.B. Han, Influence of nanosized SiC particle on the fracture toughness of ZrB_2-based nanocomposite ceramic, Mater Sci. Eng. A 527 (2010) 2925–2928.

[6] G.L. Zhao, C.Z. Huang, H.L. Liu, B. Zou, H.T. Zhu, J. Wang, Preparation of in-situ growth TaC whiskers toughening Al_2O_3 ceramic matrix composite, Int. J. Refract. Met. Hard Mater. 36 (2013) 122–125.

[7] X.H. Zhang, C.X. Liu, M.S. Li, J.H. Zhang, Research on toughening mechanisms of alumina matrix ceramic composite materials improved by rare earth additive, J. Rare Earths 26 (2008) 367–370.

[8] R.Z. Chen, W.H. Tuan, Pressureless sintering of Al_2O_3/Ni nanocomposites, J. Eur. Ceram. Soc. 19 (1999) 463–468.

[9] Y. Ji, J.A. Yeomans, Processing and mechanical properties of Al_2O_3-5 vol% Cr nanocomposites, J. Eur. Ceram. Soc. 22 (2002) 1927–1936.

[10] J.S. Lin, Y. Miyamoto, K. Tanihata, Toughening effects of WC/Co particles and compressive surface stress on (Al_2O_3–WC/Co)/TiC/Ni graded materials, J. Mater. Sci. 33 (1998) 869–876.

[11] L. Zhu, L.M. Luo, J. Li, Y.C. Wu, The influence of powder characteristics on mechanical properties of Al_2O_3–TiC–Co ceramic materials prepared by Co-coated Al_2O_3/TiC powders, Int. J. Refract. Met. Hard Mater 34 (2012) 61–65.

[12] J. Li, J.L. Sun, L.P. Huang, Effects of ductile cobalt on fracture behavior of Al_2O_3–TiC ceramic, Mater. Sci. Eng. A 323 (2002) 17–20.

[13] M.L. Gu, C.Z. Huang, B. Zou, B.Q. Liu, Effect of (Ni, Mo) and TiN on the microstructure and mechanical properties of TiB_2 ceramic tool materials, Mater. Sci. Eng. A 433 (2006) 39–44.

[14] B. Zou, C.Z. Huang, J.P. Song, Z.Y. Liu, L. Liu, Y. Zhao, Effects of sintering processes on mechanical properties and microstructure of TiB_2–TiC+8 wt% nano-Ni composite ceramic cutting tool material, Mater. Sci. Eng. A 540 (2012) 235–244.

[15] R. Gonzalez, M.G. Barandika, D. Ona, J.M. Sanchez, A. Villellas, A. Valea, F. Castro, New binder phases for the consolidation of TiB_2 hard metals, Mater. Sci. Eng. A 216 (1996) 185–192.

[16] W.H. Tuan, R.J. Brook, The toughening of alumina with nickel inclusions, J. Eur. Ceram. Soc. 6 (1990) 31–37.

[17] X.D. Sun, J.A. Yeomans, Ductile phase toughened brittle materials, J. Mater. Sci. Technol. 12 (1996) 124–134.

[18] Z.B. Yin, C.Z. Huang, B. Zou, H.L. Liu, H.T. Zhu, J. Wang, Influence of cobalt additive on mechanical properties and residual stress of Al_2O_3–TiC ceramic cutting tool material, Adv. Mater. Res 500 (2012) 657–661.

[19] G.F. Mi, H.W. Wang, X.Y. Liu, Analysis of the thermal stress in the TiC/Ti_3AlC/Ti_3Al three-phase composites, Rare Met. Mater. Eng 36 (2007) 172–177.

[20] A.G. Evans, E.A. Charles, Fracture toughness determinations by indentation, J. Am. Ceram. Soc. 59 (1976) 371–372.

[21] Y.W. Kim, Y.S. Chun, T. Nishimura, High-temperature strength of silicon carbide ceramics sintered with rare-earth oxide and aluminum nitride, Acta Mater 55 (2007) 727–736.

[22] J. Zou, G.J. Zhang, C.F. Hu, High-temperature bending strength, internal friction and stiffness of ZrB_2-20 vol% SiC ceramics, J. Eur. Ceram. Soc. 32 (2012) 2519–2527.

[23] N. Kondo, Y. Suzuki, T. Miyajima, High-temperature mechanical properties of sinter-forged silicon nitride with ytterbia additive, J. Eur. Ceram. Soc. 23 (2003) 809–815.

[24] Z.B. Yin, C.Z. Huang, B. Zou, H.L. Liu, H.T. Zhu, J. Wang, High temperature mechanical properties of Al_2O_3/TiC micro-nano-composite ceramic tool materials, Ceram. Inter. 39 (2013) 8877–8883.

[25] N.W. Zhang, C.J. Huang, F.P. Kuang, Effect of a Mg promoter on the structure and catalytic performance of a Co/Mg/HZSM-5 catalyst for the partial oxidation of methane to syngas, Acta Phys. Chim. Sin. 24 (2008) 2165–2171.

[26] T. Ohji, Y.K. Jeong, Y.H. Choa, K. Niihara, Strengthening and toughening mechanisms of ceramic nanocomposites, J. Am. Ceram. Soc. 81 (1998) 1453–1460.

[27] Z.L. Xu, Elasticity Mechanics, second ed., Higher Education Press, Beijing, 1988.